Rheological Properties and Association Behavior of Mixtures of Poly[isobutyl methacrylate–(*tert*-butylamino)ethyl methacrylate] and an Ionomer in Solution

Jian Wang,[†] Dennis G. Peiffer,[‡] Wendel J. Shuely,[§] and Benjamin Chu*[,†,∥]

*Chemistry Department, State University of New York at Stony Brook,
Long Island, New York 11794-3400, Department of Materials Science and Engineering,
State University of New York at Stony Brook, Long Island, New York 11794-2275,
Exxon Research and Engineering Company, Corporate Research Science Laboratory,
Clinton Township, Route 22 East, Annandale, New Jersey 08801, and
Research Directorate, Chemical Research, Development, and Engineering Center,
Aberdeen Proving Ground, Maryland 21010-5423*

Received December 10, 1990; Revised Manuscript Received March 18, 1991

ABSTRACT: The rheological properties and association behavior for polymer–polymer complexes consisting of a random copolymer, poly[isobutyl methacrylate–(*tert*-butylamino)ethyl methacrylate] [poly(iBMA–tBAEMA)], and an ionomer, a zinc salt of sulfonated polystyrene, in polar solvents have been measured by a magnetic needle rheometer and laser light scattering. The dramatic changes in the reduced viscosity as a function of polymer composition, concentration, cosolvent quality, temperature, and shear rate were examined by using the copolymer as the reference. The aggregate structures of the copolymer and the polymer–polymer complexes at semidilute concentrations and different polymer compositions were postulated on the basis of light scattering observations. Since the polymer–polymer complexes are very effective rheological control additives, they could be useful in a wide variety of applications, such as thickening and antimisting applications.

I. Introduction

The solution behavior of polymeric materials with low levels of ionic content, such as ionomers, has been the topic of an increasing number of studies because of their effectiveness in controlling the rheology of fluids.[1–9] A dramatic change in the solution behavior could be achieved by choosing the appropriate solvent quality, solvent polarity, solute concentration, charge density, and distribution on the polymer chains. The main reason for this success is due undoubtedly to the ability of the ionic groups on the polymer chains to form intra- and intermolecular associations in both polar and nonpolar solvents. The technological application as thickening agents has been reported.[10]

A new type of polymer–polymer complex solution systems could be formulated by mixing a zinc-neutralized ionomer with a base-containing polymer in solution in order to achieve stronger intermolecular polymer interactions. The resulting charge-transfer or metal coordination type complexation produces larger aggregates and enhances the shear-thickening or shear-thinning properties of the mixed-polymer solution. The consequence of this approach has resulted in a much enhanced solution viscosity even at low polymer concentrations and a distinct thickening effect at low shear rates.[11,12] The formation of such polymer complexes in the bulk was found to be useful in the modification of bulk properties of polymer blends[13] and in the compatibilization of two otherwise incompatible polymers in the bulk.[14]

The random copolymer poly[isobutyl methacrylate–(*tert*-butylamino)ethyl methacrylate] [poly(iBMA–tBAEMA)] can be considered as an example of a scientifically interesting and technologically important base-containing polymer. It is an industrially useful material, which, for example, can be used as an additive for motor oils because of its ability to alter the rheological properties in a variety of organic solvents. A considerable body of patents concerning the preparation and the properties of this class of polymers has been reviewed.[15,16] Our recent light scattering and viscosity studies[17,18] of poly(iBMA–tBAEMA) in polar and nonpolar solvents at room temperature have revealed its aggregation behavior in most solvents over a large range of concentration from the dilute to the semidilute solution regimes.

A polymer–polymer complex could be formed by adding a small amount of a zinc-neutralized ionomer to the poly(iBMA–tBAEMA) solution.[12] The chemical structures of the polymer–polymer complex is illustrated schematically in Figure 1. A mixture of a base-containing polymer A and an acid-containing polymer B in solution could have very complex interactions. To our knowledge, very little is known on such a system that involves aprotic dipolar solvents, a high molecular weight polymeric base, and an ionomer, such as the zinc-neutralized sulfonated polystyrene (Zn–SPS).

In this article, we report rheological properties and the ion-pair controlled association behavior of mixtures of poly(iBMA–tBAEMA) and sulfonated polystyrenes containing low levels of either a transition-metal sulfonate group or the sulfonic acid group in a polar solvent. Viscosities and apparent hydrodynamic sizes of poly(iBMA–tBAEMA)/ionomer aggregates were investigated as a function of polymer composition, polymer concentration, alcohol and amine level, temperature, and shear rate. The values were compared with those from the base-containing copolymer, which acted as a reference standard.

II. Light Scattering Analysis

II.1. Static Light Scattering. The excess Rayleigh ratio, R_{vv}, for vertically polarized incident and scattered light from a dilute polymer solution at finite scattering

---

* Author to whom all correspondence should be addressed at the Chemistry Department, State University of New York at Stony Brook.

[†] Chemistry Department, SUNY at Stony Brook.

[‡] Exxon Research and Engineering Co.

[§] Aberdeen Proving Ground.

[∥] Department of Materials Science and Engineering, SUNY at Stony Brook.

0024-9297/91/2224-4349$02.50/0

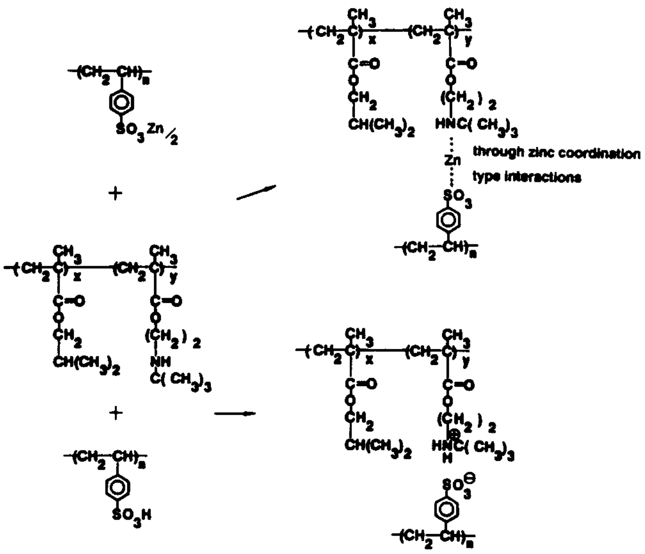

Figure 1. Schematic representation for the two types of interactions between the sulfonic acid group of Zn–SPS and the amino group on poly(iBMA–tBAEMA).

angles with $KR_g \le 1$ is given by

$$HC/R_{vv} = (1/M_w)(1 + K^2R_g^2/3) + 2A_2C \tag{1}$$

where $H = 4\pi^2n^2(\mathrm{d}n/\mathrm{d}c)^2/(N_A\lambda_0^4)$ with n, N_A, $\mathrm{d}n/\mathrm{d}c$, and λ_0 being the refractive index, Avogadro's number, the refractive index increment, and the wavelength of incident light in vacuo, respectively. A_2 is the second virial coefficient, K [$=(4\pi n/\lambda_0) \sin(\theta/2)$] is the magnitude of the scattering vector, and C is the concentration.

For semidilute polymer solutions, eq 1 can no longer hold as the polymer chains overlap. Then, the angular dependence of scattered light intensity resulting from local concentration fluctuations can be described by the relation[19,20]

$$1/R_{vv}(K) = (1/R_{vv}(0))(1 + K^2L^2/3) \tag{2}$$

where L is a correlation length. This picture was postulated on the assumption that a homogeneous transient network was formed at a concentration $C > C^*$, which may be defined as

$$C^* = M_w/N_AR_g^3 \tag{3}$$

where R_g is the radius of gyration.

II.2. Dynamic Light Scattering. The measured photoelectron count autocorrelation function in the self-beating mode has the form

$$G^{(2)}(t) = A(1 + b|g^{(1)}(t)|^2) \tag{4}$$

where A is the background (or base line), b is a parameter that accounts for the nonideal point detector, and $g^{(1)}(t)$ is the normalized first-order electric field autocorrelation function at delay time t. For a polydisperse system, $|g^{(1)}(t)|$ is related to the normalized characteristic line-width distribution function $G(\Gamma)$ given by the relation

$$|g^{(1)}(t)| = \int_0^\infty G(\Gamma)e^{-\Gamma t}\,\mathrm{d}\Gamma \tag{5}$$

where Γ is the characteristic line width. Laplace inversion of eq 5 could be accomplished by using different approaches, with the CONTIN method provided by Provencher[21,22] being the most popular. Thus, the correlation function profile analysis can provide an estimate of the hydrodynamic size and its size distribution under appropriate conditions. Unfortunately, the Laplace inversion is related to the well-known ill-conditioned problem. So, extreme caution should be taken in extracting the true information from eq 5. The average characteristic line width is defined by

$$\bar{\Gamma} = \int \Gamma G(\Gamma)\,\mathrm{d}\Gamma \tag{6}$$

with its variance being

$$\mu_2/\bar{\Gamma}^2 = \int \left(\frac{\Gamma - \bar{\Gamma}}{\bar{\Gamma}}\right)^2 G(\Gamma)\,\mathrm{d}\Gamma \tag{7}$$

By extrapolating $\bar{\Gamma}/K^2$ to zero K, we could determine the Z-average translational diffusion coefficient D_0 ($= \lim_{K\to 0} \bar{\Gamma}/K^2$) at concentration C within the dilute-solution regime. An application of the Stokes–Einstein equation yields an apparent hydrodynamic radius

$$R_h = kT/(6\pi\eta_0D_0) \tag{8}$$

where η_0 is the solvent viscosity and kT is the thermal energy.

In a semidilute solution, one can expect at least two kinds of molecular motion, i.e., cooperative motion of the entangled chains described by a cooperative diffusion coefficient D_{co} ($=\lim_{K\to 0} \bar{\Gamma}_{fast}/K^2$) and the translational motion of individual molecules in the entangled network as described by a slower translational diffusion coefficient. de Gennes has provided a relation for semidilute solutions[20]

$$D_{co} \approx kT/(6\pi\eta_0\xi) \tag{9}$$

where ξ is the dynamic correlation length. In the above discussion, the equations are valid only for homopolymers. In the case of copolymers and polymer–polymer complexes, the parameters become apparent ones, useful for qualitative consideration at best.

III. Experimental Section

III.1. Samples. The random copolymer poly(iBMA–tBAEMA) (lot no. CM1-120) was prepared by emulsion polymerization and purchased from Polyscience. The lot investigated was obtained from the latex-phase blend of several independent emulsion polymerizations. Aqueous size-exclusion chromatography (SEC) and light scattering measurements in isopropylamine (IPA)[17] provided an estimate of the copolymer weight-average molecular weight to be 2.7×10^6 and 2.4×10^6, respectively. The copolymer showed a broad molecular weight distribution typical of free-radical polymerization processes. The molar ratio of iBMA to tBAEMA was 77:23 as determined by ^{13}C NMR.

The free acid sulfonated polystyrene (H–SPS) and zinc salt form of sulfonated polystyrene (Zn–SPS) were prepared from the anionically polymerized polystyrene with a weight-average molecular weight of 1.05×10^5. The preparation of these ionomers has been described in ref 23. The sulfur content for both acid and zinc salt forms was 4.7 mol % as determined by the Dietert sulfur analysis.

All the solvents, *N,N*-dimethylacetamide (DMAA), *N*-methylbutylamine, and 1-butanol, were purchased from the Aldrich Chemical Co. and redistilled before use. Stock solutions were prepared volumetrically by dissolving separately each sample in DMAA at 50 °C with occasional agitation for a couple of weeks and then keeping it at room temperatures for another week. The solutions of poly(iBMA–tBAEMA)/ionomer were prepared by dropwise addition of the homogeneous solutions of Zn–SPS to the stirred poly(iBMA–tBAEMA) solutions. Solutions of the polymer mixture were then kept at room temperature with occasional agitation for 5 days in order to ensure that the solution mixtures were equilibrated.

III.2. Viscosity Measurement. Viscosity measurements were performed mainly by using a magnetic sphere/needle rheometer,[24,25] which permitted precise measurements (say, a standard deviation of ~3% when conducted on the same polymer

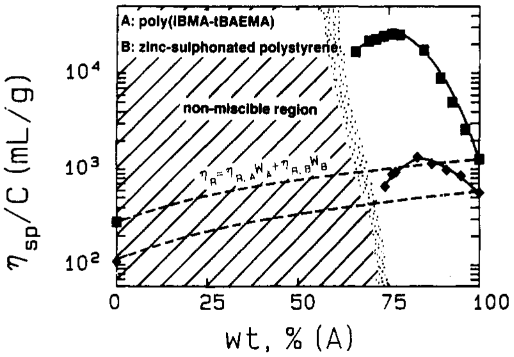

Figure 2. Reduced viscosity–polymer composition diagram for a mixture of poly(iBMA–tBAEMA) and Zn–SPS in DMAA at 30 °C. The total polymer concentration $C = 1.00 \times 10^{-2}$ g/mL (solid diamonds) and $C = 3.00 \times 10^{-2}$ g/mL (solid squares). The shadowed area with a smeared boundary in polymer composition, which reflects the uncertainty of phase-separation thresholds, represents the nonmiscible region where a gellike precipitate is formed. The two dashed lines denote the theoretical linear additivity of the reduced viscosity for a binary polymer solution without interpolymer interactions.

solution) over a viscosity range from 0.7 to 1×10^5 cP and a shear rate range of about 1×10^{-2} – 1×10^1 s^{-1}. Temperature was controlled to ±0.01 °C by using a water bath circulator. In most cases, the viscosity values were converted into the reduced viscosity defined by $\eta_{sp}/C = (\eta - \eta_0)/(\eta_0 C)$, where η_0 is the solvent viscosity and η is the solution viscosity at concentration C.

III.3. Light Scattering. A Spectra Physics Model 165 argon ion laser operated at $\lambda = 488$ nm and an output power of 0.1 W was used as the light source. The sample holder was thermostated to ±0.01 °C over a temperature range from room temperature to ~100 °C. A standard photon counter and a Brookhaven Instruments BI2030 128-channel digital autocorrelator were used to perform light scattering intensity and time correlation function measurements over an angular range of 15–135°.

IV. Results and Discussion

IV.1. Rheological Properties. IV.1.1. Composition and Concentration Dependence. Interpolymer interactions in a binary polymer solution between polymer A containing basic groups and polymer B containing acidic groups could take place and give rise to noncovalent association and cross-linking among polymer A and polymer B as a result of the acid–base pair attractions. The polymer molecules would tend to form clusters or networks. The enhanced association can, if controllable, lead to an increase in the viscosity, while excessive cross-linking would lead to localized polymer gel formation in solution. The clustering of binary polymers in solution could be achieved by using an appropriate mixing recipe for poly(iBMA–tBAEMA) and Zn–SPS. Figure 2 shows reduced viscosity–polymer composition diagrams for the mixture of poly(iBMA–tBAEMA) (polymer A) and Zn–SPS (polymer B) at a total concentration of 1.00×10^{-2} g/mL (solid diamonds) and 3.00×10^{-2} g/mL (solid squares) in DMAA at 30 °C. DMAA is a good solvent for both polymer A and polymer B at 30 °C, with the reduced viscosity for polymer A and polymer B being ~5.7×10^2 and 1.1×10^2 mL/g, respectively. Upon mixing of two pure A and pure B solutions, gel-like precipitates were observed over a very broad range in the polymer composition, as schematically shown by the shadowed area with a smeared boundary in composition in Figure 2. This uncertainty accounts for the complex cross-linking kinetics and the difficulty in determining the accurate phase separation thresholds. The precipitates were found to be essentially insoluble in DMAA at room temperature, suggesting the formation of localized and highly cross-linked polymer networks. It should be noted that the whole solution never formed a uniform gel in the nonmiscible region. This could be understood as a kinetic consequence of uneven local cross-linking. The dashed lines between the reduced viscosity values of pure A and of pure B as illustrated in Figure 2 represent the hypothetical reduced viscosity of the polymer solution without interactions between polymer A and polymer B. The reduced viscosity of polymer mixtures in solution exhibits a peak that shifts toward a lower weight fraction of polymer A from 83% to 75%, with increasing total polymer concentration from 1×10^{-2} to 3×10^{-2} g/mL. The reduced viscosity in this region is significantly altered by the interpolymer interactions according to the mixing ratio. For $C = 3 \times 10^{-2}$ g/mL, the reduced viscosity is increased by a factor of 20 at the maximum as compared with that of pure A. In the upper limit, if all the sulfonic groups on polymer B had been used up to react with the basic groups on polymer A, only a few percent of the basic groups on the poly(iBMA–tBAEMA) chains would have reacted at the maximum reduced viscosity. However, in reality, the extent of the interaction should be much less because the two polymer backbones (iBMA and PS) are not compatible. The maximum suggests a most effective polymer composition for the mixture of poly(iBMA–tBAEMA)/(4.7 mol %) Zn–SPS in DMAA in order to achieve a thickening effect at room temperature with a minimum amount of *total* polymer additive.

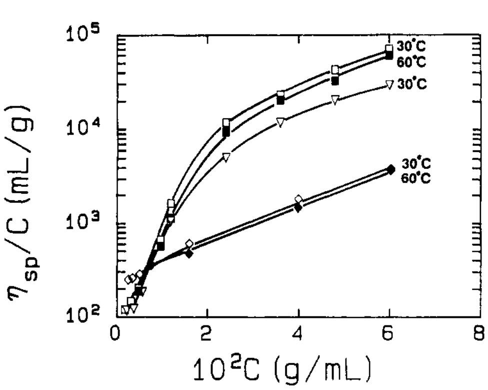

Figure 3. Reduced viscosity–concentration profiles of poly(iBMA–tBAEMA) (diamonds), of a mixture of poly(iBMA–tBAEMA)/Zn–SPS at a mixing ratio of 4:1 (w/w) (squares), and of a mixture of poly(iBMA–tBAEMA)/H–SPS at a mixing ratio of 4:1 (w/w) (hollow inverse triangles) in DMAA.

The concentration dependence of the reduced viscosity for the mixtures of poly(iBMA–tBAEMA)/Zn–SPS and of poly(iBMA–tBAEMA)/H–SPS in DMAA at a copolymer/ionomer mixing ratio of 4:1 (w/w) is shown in Figure 3. The mixture solutions poly(iBMA–tBAEMA)/Zn–SPS (hollow squares and solid squares at 30 and 60 °C, respectively) and poly(iBMA–tBAEMA)/H–SPS) (hollow inverse triangles) show a sharper increase in the reduced viscosity with increasing concentration when compared with the curves for the pure poly(iBMA–tBAEMA) (hollow diamonds and solid diamonds at 30 and 60 °C, respectively). The poly(iBMA–tBAEMA)/Zn–SPS solution shows a larger viscosity enhancement effect than poly(iBMA–tBAEMA)/H–SPS solution as the total polymer concentration is raised to ~7.0×10^{-3} g/mL. This indicates the existence of charge-transfer complexation involving an intermediary zinc ion with a nitrogen of one chain and a sulfonate group of another chain. In particular, a crossover of the curves between the mixtures and pure poly(iBMA–tBAEMA) at a very low total polymer concentration (~7.0×10^{-3} g/mL) is clearly demonstrated.

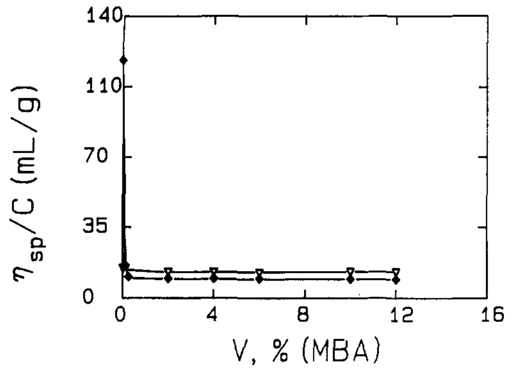

Figure 4. Reduced viscosity of poly(iBMA–tBAEMA) (hollow reverse triangles) and of a mixture of poly(iBMA–tBAEMA)/Zn–SPS (solid diamonds) at a mixing ratio of 4:1 (w/w), $C = 2.00 \times 10^{-2}$ g/mL and 30 °C in DMAA with diffferent levels of *N*-methylbutylamine. A strong downward jump in the reduced viscosity of the mixture of poly(iBMA–tBAEMA)/Zn–SPS at close to zero level of *N*-methylbutylamine signifies the collapse of cross-linking by acid–base pair interactions between polymer chains.

Below this point, both mixtures show an even lower reduced viscosity than that of the pure poly(iBMA–tBAEMA). The ionomer (Zn–SPS or H–SPS), when prevented from functioning as a linking agent, can decrease the reduced viscosity of the poly(iBMA–tBAEMA) solution since both ionomers have a relatively low average molecular weight and would essentially act as diluents.

At a total polymer concentration of ~0.05 g/mL and 30 °C the reduced viscosity of solution mixtures, poly(iBMA–tBAEMA)/Zn–SPS and poly(iBMA–tBAEMA)/H–SPS, is about 18 and 8 times that of a poly(iBMA–tBAEMA) solution, respectively.

IV.1.2. Amine and Alcohol Effect. The influence of an amine, *N*-methylbutylamine, on the reduced viscosity of poly(iBMA–tBAEMA) (hollow inverse triangles) and of a polymer mixture, poly(iBMA–tBAEMA)/Zn–SPS (solid diamonds), in DMAA is shown in Figure 4. For the pure poly(iBMA–tBAEMA) solution, the addition of *N*-methylbutylamine did not substantially affect the reduced viscosity. However, by just adding a small amount of amine, the reduced viscosity of poly(iBMA–tBAEMA)/Zn–SPS was sharply decreased to a value comparable to that of pure poly(iBMA–tBAEMA). This observation clearly indicates that amines are able to break up these types of polymer–polymer complexes due to their "titrating" effect on the sulfonic groups. It renders a useful way of dissociating the interpolymer complexes and could be useful in special technological applications.

The influence of an alcohol, 1-butanol, on the reduced viscosity of poly(iBMA–tBAEMA) and of poly(iBMA–tBAEMA)/Zn–SPS was measured. The reduced viscosity remained unchanged for both cases with the cosolvent composition containing up to 25% (by volume) of the alcohol. It was reported that alcohol could "trap" sulfonic groups and consequently break up the ionic aggregates.[2] In our case, no appreciable change in the reduced viscosity was observed by introducing an alcohol to the solution, suggesting that the acid–base pair controlled association species are more favored than the alcohol-trapped species (alcohol–Zn–SPS). This behavior is consistent with the fact that alcohol is a weaker "acid" than the sulfonic acid. Therefore, there is no reason to anticipate an appreciable effect by an alcohol on the reduced viscosity for these types of interpolymer complexes.

IV.1.3. Temperature and Shear Rate Dependence. Figure 5 shows a comparison of the temperature effect on the reduced viscosity of poly(iBMA–tBAEMA) (hollow diamond) and of a polymer mixture of poly(iBMA–tBAEMA)/Zn–SPS (hollow inverse triangles) over a temperature range of 25–75 °C in DMAA. The poly(iBMA–tBAEMA)/Zn–SPS solution shows a slight decrease in the reduced viscosity with increasing temperature, while the poly(iBMA–tBAEMA) solution remains essentially unchanged. The same phenomenon was also observed in the experiment of the concentration dependence at different temperatures as shown in Figure 3. It is sufficient to say that the interpolymer complex structures are not significantly changed by thermal energies upon heating to 75 °C. The strength of the interpolymer associates via ion-pair interactions could be very strong. The activation energy, ΔE, calculated by using the Arrhenius equation for the mixture and the pure polymer solution is 4.3 and 2.9 kcal/mol, respectively.

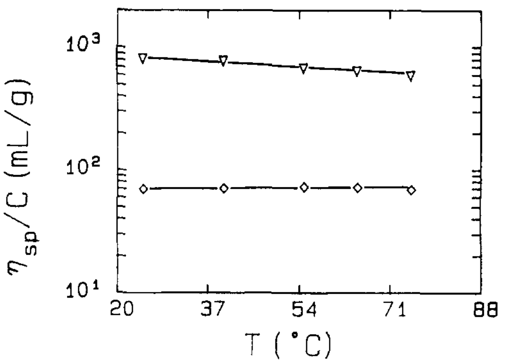

Figure 5. Temperature effect on the reduced viscosity of poly(iBMA–tBAEMA) (hollow inverse triangles) and of a mixture of poly(iBMA–tBAEMA)/Zn–SPS (hollow diamonds) at a mixing ratio of 4:1 (w/w) in DMAA at $C = 4.00 \times 10^{-2}$ g/mL.

Figure 6a shows the shear rate dependence of the viscosity for the solutions of a mixture of poly(iBMA–tBAEMA)/Zn–SPS (hollow diamonds) and of poly(iBMA–tBAEMA) (hollow inverse triangles) at $C = 6.00 \times 10^{-2}$ g/mL in DMAA at 30 °C. It is obvious that the non-Newtonian behavior for the polymer mixture solution appears at a lower shear rate when compared with that for the pure polymer solution. Moreover, it should be noted that this polymer mixture displays a shear-thinning effect, ie., a dramatic decrease in viscosity at shear rates higher than 1 s^{-1}. The power law coefficients α, which is defined by $\eta(\dot{\gamma})/\eta(\dot{\gamma} = 0) \sim \dot{\gamma}^{-\alpha}$, in a log–log plot of $\eta(\dot{\gamma})/\eta(\dot{\gamma} = 0)$ versus γ (s^{-1}), were estimated. On the basis of the three high shear data points, $\alpha = 1.14 \times 10^{-2}$ and 7.30×10^{-2} for poly(iBMA–tBAEMA) and poly(iBMA–tBAEMA)/Zn–SPS, respectively.

The viscosity of this mixture at $C = 1.00 \times 10^{-2}$ g/mL was also measured by a Brookfield viscometer, which allowed the operation at higher shear rates in order to check whether shear thickening could exist at certain higher shear rates as reported for a similar system.[11] The result is shown in Figure 6b. The viscosity goes down continuously with increasing shear rate and reaches a stationary value. No shear thickening was observed throughout the shear rate region studied.

IV.2. Molecular Conformation of the Polymer–Polymer Complex. Figure 7 shows a plot of the excess scattered intensity after extrapolation to $\theta = 0$ for poly(iBMA–tBAEMA)/Zn–SPS against the polymer composition in DMAA at a fixed concentration of 1.00×10^{-2} g/mL. This experiment demonstrates that the excess scattered intensity first increases with increasing ionomer content, reaches a maximum value at an ionomer content of ~17% (by weight), and decreases slightly with a further increase in the ionomer content. The primary

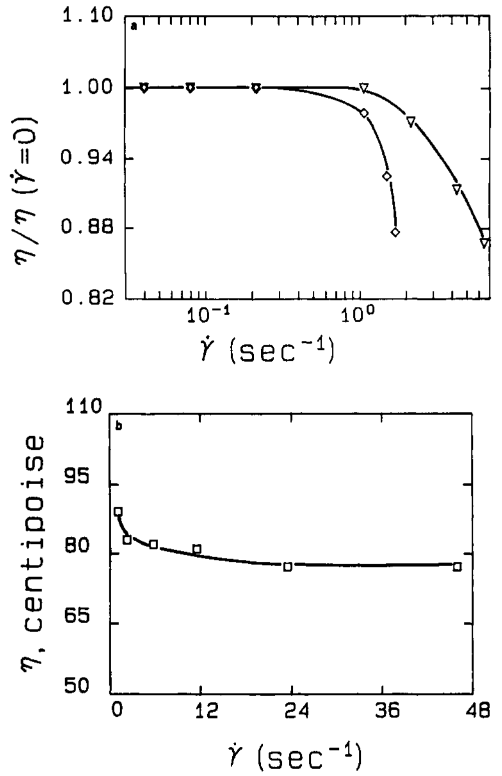

Figure 6. (a) Shear rate dependence of viscosity normalized to zero shear rate for poly(iBMA-tBAEMA) (hollow inverse triangles) and for a mixture of poly(iBMA-tBAEMA)/Zn-SPS at a mixing ratio of 4:1 (w/w) in DMAA at $C = 6.00 \times 10^{-2}$ g/mL and 30 °C. (b) Shear rate dependence of viscosity for a mixture of poly(iBMA-tBAEMA)/Zn-SPS = 4:1 (w/w) at $C = 2.20 \times 10^{-2}$ g/mL and higher shear rates.

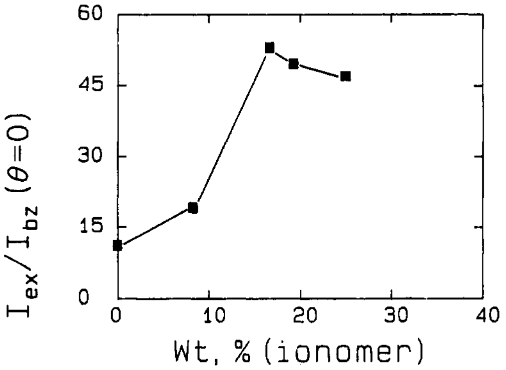

Figure 7. Normalized excess intensity after extrapolation to $\theta = 0$ for a mixture of poly(iBMA-tBAEMA)/Zn-SPS versus polymer composition in DMAA at $C = 1.00 \times 10^{-2}$ g/mL and 30 °C. The maximum appearing at ~17% of Zn-SPS is in reasonable agreement with the reduced viscosity-composition diagram (see Figure 2).

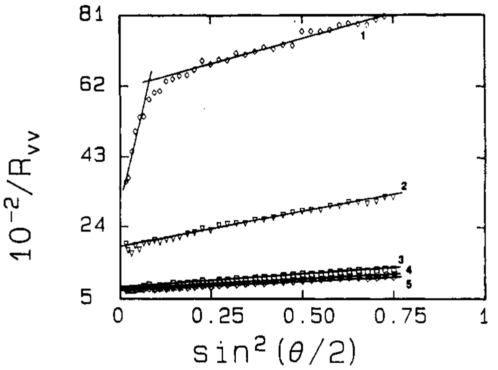

Figure 8. Plots of the reciprocal of the Rayleigh ratio versus $\sin^2(\theta/2)$ for the mixtures of poly(iBMA-tBAEMA)/Zn-SPS at a weight fraction of poly(iBMA-tBAEMA) of (1) 100%, (2) 91.7%, (3) 83.3%, (4) 80.7%, and (5) 75.0% in DMAA at a total polymer concentration $C = 1.00 \times 10^{-2}$ g/mL and 30 °C. The correlation length L was estimated from the slopes for each curve to be 158 and 33 nm in the low-angle and high-angle regimes of curve 1 and 49, 62, 42, and 41 nm for curves 2–5, respectively, based on the relation $1/R_{vv}(K) = (1/R_{vv}(0))(1 + K^2L^2/3)$.

factor responsible for the significant change in the excess scattered intensity at $\theta = 0$ from the polymer–polymer complex solutions could be attributed to the variation in the cluster size. Here, we denote an increase in $I_{ex}(\theta{=}0)$ as an increase in the aggregate molar mass. The presence of a maximum in the excess scattered intensity signifies the formation of possibly the largest cluster size in this family near ~17% (by weight) of the ionomer content. This observation is in agreement with the viscosity measurements. In spite of the complexity in light scattering measurements of copolymer complexes, the qualitative observation of the maximum in $I_{ex}(\theta{=}0)$ has strengthened the observation that the most effective polymer composition for our present system as a rheology enhancement agent is to use ~17 wt % Zn-SPS in the poly(iBMA-tBAEMA) solution at $C = 1 \times 10^{-2}$ g/mL.

Figure 8 shows plots of the angular dependence of the reciprocal of the Rayleigh ratio for poly(iBMA-tBAEMA)/Zn-SPS in DMAA at a fixed total polymer concentration of 1×10^{-2} g/mL and varying polymer composition ratios. It should be noted that the analysis of the scattering behavior for such a polymer–polymer complex at semidilute concentrations ($C/C^* \sim 3$) could be considered only qualitatively at best. The scattering curves can be distinguished into two types. Curve 1, which represents the angular distribution of scattered intensity from the poly(iBMA-tBAEMA) solution, manifests two linear sections that have different slopes, while the other curves, which represent the poly(iBMA-tBAEMA)/Zn-SPS solutions at differing ionomer content, show essentially a single linear distribution. The first type of scattering curve with two slopes is commonly seen in semidilute polymer solutions.[26] The correlation length for curve 1 via eq 2 shows the two separate slopes. They are 158 and 33 nm for the low- and high-K-range sections, respectively. The low-angle behavior suggested the presence of large inhomogeneities. For curves 2–4, correlation lengths of 49, 62, 42, and 41 nm for curves 2–5, respectively, were estimated. At ~17 wt % Zn-SPS, the polymer mixture had the most expanded mesh size (62 nm) and therefore the highest reduced viscosity. At other ionomer concentrations, the cross-linking has not been optimized. For the pure poly(iBMA-tBAEMA) solution the large inhomogeneities do not contribute appreciably to the viscosity enhancement.

Figure 9 shows the intensity–intensity time correlation functions for the mixtures of poly(iBMA-tBAEMA)/Zn-SPS at different polymer compositions of (1) 100%, (2) 91.7%, (3) 83.3%, (4) 80.7%, and (5) 75.0% of poly(iBMA-tBAEMA) by weight in DMAA and at a total polymer concentration $C = 1.00 \times 10^{-2}$ g/mL and $\theta = 35°$. Apparently, curve 1 for the pure copolymer solution demonstrates a deviation from single-exponential behavior: a fast mode and a slow mode appear at $C > C^*$. The two modes are responsible for the two slopes of the half-logarithm correlation function for curve 1 and reinforce the observation for curve 1 in Figure 8. It is interesting to note that the other curves for the polymer–polymer complex solutions show essentially unimodal behavior. Laplace inversion of these correlation functions was performed by using the CONTIN method.[21,22] The values are listed in Table I.

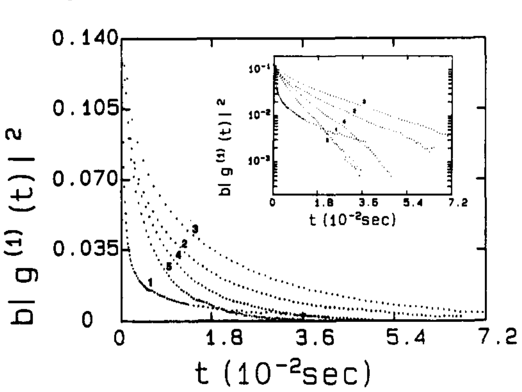

Figure 9. Measured net intensity–intensity time correlation functions for mixtures of poly(iBMA–tBAEMA) and Zn–SPS at a weight fraction of poly(iBMA–tBAEMA) of (1) 100%, (2) 91.7%, (3) 83.3%, (4) 80.7%, and (5) 75.0% in DMAA at a total polymer concentration $C = 1.00 \times 10^{-2}$ g/mL, $\theta = 45°$, and 30 °C. The inset shows the semilog plots of these correlation functions, where curve 1 shows bimodal motions, while the rest of the curves show essentially unimodal motions.

Table I
Correlation Function Profile Analysis of Solution Mixtures of Poly(iBMA–tBAEMA)/Zn–SPS at Different Polymer Compositions in DMAA at 30 °C by the CONTIN Method[a]

	1	2	3	4	5
wt % (A)	100	91.7	83.3	80.7	75.0
θ, deg	35	35	35	35	35
$\bar{\Gamma}_1[\bar{\Gamma}_2]$, s^{-1}	98 [1681]	42	30	56	91
$\mu_2/\bar{\Gamma}_1^2[\mu_2/\bar{\Gamma}_2^2]$	0.73 [0.22]	0.24	0.22	0.06	0.18
$S_1[S_2]$	0.40 [0.60]				
$\xi_1(\bar{\Gamma}_1)[\xi_2(\bar{\Gamma}_2)]$, nm	∞ [22]	1176	1392	611	455

[a] A is poly(iBMA–tBAEMA); $C = 1.00 \times 10^{-2}$ g/mL. $\xi = kT/(6\pi\eta_0 D_0(C))$ where $D_0(C) = \lim_{K\to 0} \bar{\Gamma}/K^2$.

After extrapolation of $\bar{\Gamma}/K^2$ to $K = 0$, the diffusion coefficient $D_0(C)$ $[=\bar{\Gamma}/K^2(\theta=0)]$ and the dynamic correlation length can be estimated. In polymer–polymer complex solutions, $\xi \sim 1400$ nm at wt % (A) = 0.83, which is ~10 times the value of R_h for poly(iBMA–tBAEMA) in DMAA in the dilute-solution regime.[17] It could be seen from the variance in Table I that, in spite of the disparity in the molar mass between the consitituents of the ionic polymer complex, the length distribution is not very broad. We could perhaps attribute the narrower size distribution to the nonspecific intermolecular interactions among the copolymer and the ionomer, except that the cross-linking took place near the surface of the polymer coils. Thus, the smaller coils might have a more effective surface per unit volume for the intermolecular interactions, resulting in a more uniform size distribution in the polymer complex. It should be emphasized that in our discussion we should not take the absolute magnitude of L and ξ seriously. They are being used as guides to illustrate the complex association behavior of the polymer–polymer complexation. The introduction of extensive "cross-linking" in a semidilute solution clearly destroys the desired loose network and forms more compact clusters, which are not effective in enhancing the fluid viscosity.

Possible structures for semidilute solutions of poly(iBMA-tBAEMA) and poly(iBMA-tBAEMA)/Zn–SPS might be that a transient network with large inhomogeneities of pure poly(iBMA–tBAEMA) is altered into cross-linked clusters having an expanded mesh size by additional polymer intermolecular interactions among the acid–base pairs after addition of a small amount of the ionomer. The electrostatic attractive force between the opposite ion pairs would be viewed as responsible for this dramatic structural change. Apparently, the uneasy-slip-away structure of ion-pair-controlled clusters could contribute much more to the viscosity than the easy-slip-away transient network. The relative strength of the clustering links is another important factor of the polymer–polymer complexes that may determine the shear-thickening or shear-thinning properties.

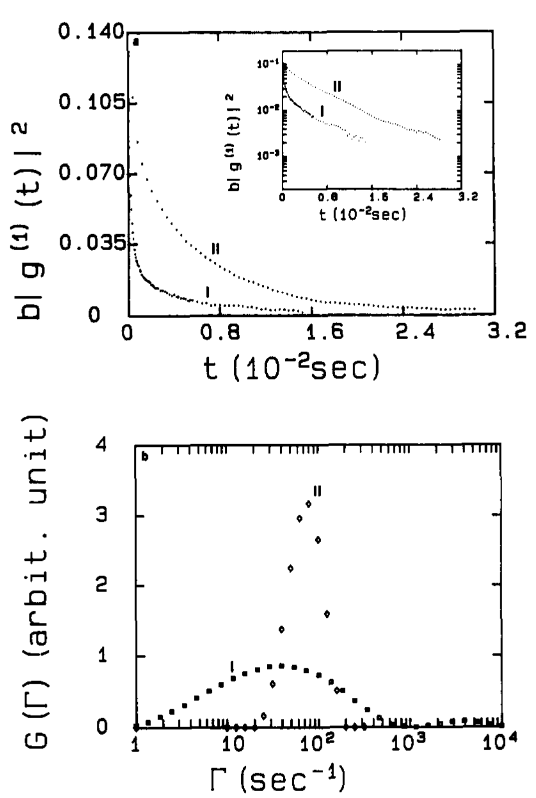

Figure 10. (a) Measured net intensity–intensity time correlation functions for poly(iBMA–tBAEMA)(I) and for poly(iBMA–tBAEMA)/Zn–SPS with a weight fraction of 83.3% of poly(iBMA–tBAEMA) (II) in DMAA at $C = 1.00 \times 10^{-2}$ g/mL and 82 °C. The inset shows the semilog plots of the two correlation functions, showing still bimodal behavior for poly(iBMA–tBAEMA) and single exponential behavior for poly(iBMA–tBAEMA)/Zn–SPS at such a high temperature. (b) Corresponding distribution functions of the characteristic line width from the CONTIN method.

Figure 10a shows the influence of higher temperature on the correlation functions for poly(iBMA–tBAEMA) (I) and poly(iBMA–tBAEMA)/Zn–SPS (II) with a weight fraction of 83.3% of poly(iBMA–tBAEMA) at a fixed concentration. Again, a bimodal diffusion for the pure poly(iBMA–tBAEMA) and a unimodal diffusion for poly(iBMA–tBAEMA)/Zn–SPS as clearly evidenced in the inset were observed at 82 °C. The corresponding characteristic line-width distributions are shown in the Figure 10b. For poly(iBMA–tBAEMA), the first peak corresponds to the slow mode with $\bar{\Gamma}_1 = 186$ s^{-1} and the normalized integrated amplitude $S_1 = 0.38$. The second peak is related to the fast mode with $\bar{\Gamma}_2 = 4.76 \times 10^3$ s^{-1} and $S_2 = 0.62$. The fast mode had a slight angular dependence and possessed a correlation length of 13 nm, which was ~2 times smaller than that at 30 °C (see Table I). The slow mode had a pronounced angular dependence and its apparent translational diffusion coefficient D_0 $(=\bar{\Gamma}_2/K^2(\theta=0))$ tended to move toward zero in the extrapolation to $K = 0$. Interestingly, the integrated amplitude ratio of the fast mode to the slow mode, S_2/S_1, for poly(iBMA–tBAEMA) was not influenced substantially upon heating to 82 °C. For the poly(iBMA–tBAEMA)/Zn–SPS the single broad peak had $\bar{\Gamma} = 90$ s^{-1} and a variance of 0.15. The dynamic correlation length could be estimated to be 1.11×10^3 nm, which was slightly smaller than that at 30 °C, again in agreement with the reduced viscosity measurements. The temperature resistance to viscosity changes could be viewed as another advantage for this type of interpolymer complexes.

V. Conclusion

The ion-pair-controlled polymer-polymer complexes, poly(iBMA-tBAEMA)/Zn-SPS, in organic solvents were developed in order to achieve an extraordinary enhancement in the thickening efficiency. Shear-thickening/thinning properties could now be manipulated by the introduction of additional forces, which could influence not only the static but also the dynamics of entangled polymer complexes in solution. The viscosity of the poly(iBMA-tBAEMA)/Zn-SPS solutions is dependent on the polymer composition, concentration, temperature, and shear rate. A maximum in the reduced viscosity versus polymer composition was found to shift from 83% to 75% of poly(iBMA-tBAEMA) by weight for a 4.7 mol % Zn-SPS with an increase in concentration from 1×10^{-2} to 3×10^{-2} g/mL in DMAA, providing a most effective clustering in solution without observable microgel formation. A broad region in the polymer composition for the gel-like precipitate was observed at weight fractions of poly(iBMA-tBAEMA) $\leq$ 70% in DMAA at room temperatures. The reduced viscosity of poly(iBMA-tBAEMA)/Zn-SPS could be raised as much as 20 times higher than that of poly(iBMA-tBAEMA) in DMAA at a total polymer concentration of $C \sim 0.03$ g/mL. The mixture of poly(iBMA-tBAEMA)/Zn-SPS shows a more pronounced shear-thinning effect than that of poly(iBMA-tBAEMA) in the shear rate range we have covered. The addition of an alcohol and an amine to the mixture solution plays substantially different roles, i.e., no appreciable effect on the cluster size in the former case, while total destruction to the polymer complex formation due to the titrating ability of the amine on the sulfonic ionic group in the latter.

Measurements of excess scattered intensity from interpolymer complex solutions at a fixed polymer concentration have further confirmed the fact that the most effective clustering composition as observed in the viscosity measurements can also be explained qualitatively from light scattering experiments. The aggregates are formed by interpolymer coils, which do not penetrate extensively. These interpolymer complexes have narrower length distributions when compared with the length distributions of the individual components and are resistant to temperature variations up to at least 82 °C, the highest temperature at which we have studied.

It should also be noted that dramatic changes in the physical properties of these interpolymer complexes are anticipated with changes in the tBAEMA composition in the base-containing copolymer (or the sulfonate content within the ionomer).

Acknowledgment. B.C. acknowledges the support of this research by the U.S. Army Research Office (DAAL0391G0040) and the Department of Energy (DEFG0286ER45237A005).

References and Notes

(1) Eisenberg, A.; King, M. *Ion Containing Polymer*; Academic Press: New York, 1977.
(2) Lundberg, R. D.; Makowski, H. S. *J. Polym. Sci. Polym. Phys. Ed.* 1980, *18*, 1821.
(3) Lundberg, R. D.; Phillips, R. R. *J. Polym. Sci., Polym. Phys. Ed.* 1982, *20*, 1143.
(4) Peiffer, D. G.; Lundberg, R. D. *Polymer* 1983, *24*, 300.
(5) Lundberg, R. D.; Phillips, R. R. *J. Polym. Sci., Polym. Lett. Ed.* 1984, *22*, 377.
(6) Hara, M.; Win, J. L. *Macromolecules* 1986, *19*, 2887.
(7) Hara, M.; Lee, A. H.; Wu, J. *J. Polym. Sci., Polym. Phys. Ed.* 1987, *25*, 1409.
(8) Peiffer, D. G.; Kaladas, J.; Duvdevani, I.; Higgins, J. S. *Macromolecules* 1987, *20*, 1397.
(9) Hara, M.; Wu, J. L.; Lee, A. H. *Macromolecules* 1988, *21*, 2214.
(10) Thaler, W. A.; Walker, T. O.; Lundberg, R. D.; Wagensommer, J. (Exxon Research and Engineering Co.) U.S. Patent 4,442,011, 1984.
(11) Lundberg, R. D.; Peiffer, D. G.; Phillips, R. R. U.S. Patent 4,617,337, 1986.
(12) Chu, B.; Wang, J.; Peiffer, D. G.; Shuely, W. J. *Macromolecules*, in press.
(13) Peiffer, D. G.; Agarwal, P. K.; Duvdevani, I.; Lundberg, R. D. *Plast. Eng.* 1987, *43*, 35.
(14) Eisenberg, A.; Smith, P.; Zhous, Z. L. *Polym. Eng. Sci.* 1982, *22*, 1117.
(15) Hong, S. H.; McHugh, V. M. Review of polymerization and properties of aminoalkyl acrylates and aminoalkyl methacrylates. Government Report CRDEC-TR-88092, July 1987; with 31 references.
(16) Hong, S. H.; McHugh, V. M. Review of preparation and properties of polymers from copolymerization of aprotic acrylic monomers with protic acrylic monomers. Government Report CRDEC-TR-88093, July 1988; with 57 references.
(17) Chu, B.; Wang, J.; Shuely, W. J. *Macromolecules* 1990, *23*, 2252.
(18) Chu, B.; Wang, J.; Shuely, W. J. *Polymer* 1990, *31*, 805.
(19) Edwards, S. F. *Proc. Phys. Soc., London* 1985, *83*, 5293.
(20) de Gennes, P.-G. *Scaling Concepts in Polymer Physics*; Cornell University: Ithaca, NY, 1979.
(21) Provencher, S. W. *Biophys. J.* 1976, *16*, 27; *J. Chem. Phys.* 1976, *64*, 2772; *Makromol. Chem.* 1979, *180*, 201.
(22) Version 2, March 1984, courtesy of S. W. Provencher.
(23) Gabrys, B.; Higgins, J. S.; Lantman, C. W.; MacKnight, W. J.; Pedley, A. M.; Peiffer, D. G.; Rennie, A. R. *Macromolecules* 1989, *22*, 3746.
(24) Hilfiker, R.; Chu, B.; Shook, J. *Rev. Sci. Instrum.* 1989, *60*, 760.
(25) Chu, B.; Hilfiker, R. *Rev. Sci. Instrum.* 1989, *60*, 3047.
(26) Huber, K.; Bantle, S.; Burchard, W.; Fetters, L. J. *Macromolecules* 1986, *19*, 1404.